

AperTO - Archivio Istituzionale Open Access dell'Università di Torino

## Investigating the 2nd knee: The KASCADE-grande experiment

**This is a pre print version of the following article:**

*Original Citation:*

*Availability:*

This version is available <http://hdl.handle.net/2318/126056> since 2023-02-03T11:29:52Z

*Published version:*

DOI:10.1088/1742-6596/47/1/029

*Terms of use:*

Open Access

Anyone can freely access the full text of works made available as "Open Access". Works made available under a Creative Commons license can be used according to the terms and conditions of said license. Use of all other works requires consent of the right holder (author or publisher) if not exempted from copyright protection by the applicable law.

(Article begins on next page)

# Investigating the 2<sup>nd</sup> knee: The KASCADE-Grande experiment

A. Haungs<sup>\*</sup>, W.D. Apel<sup>\*</sup>, F. Badea<sup>\*,1</sup>, K. Bekk<sup>\*</sup>, A. Bercuci<sup>†</sup>,  
 M. Bertaina<sup>‡</sup>, J. Blümer<sup>\*,§</sup>, H. Bozdog<sup>\*</sup>, I.M. Brancus<sup>†</sup>,  
 M. Brüggemann<sup>¶</sup>, P. Buchholz<sup>¶</sup>, A. Chiavassa<sup>‡</sup>, K. Daumiller<sup>\*</sup>,  
 F. Di Pierro<sup>‡</sup>, P. Doll<sup>\*</sup>, R. Engel<sup>\*</sup>, J. Engler<sup>\*</sup>, P.L. Ghia<sup>||</sup>, H.J. Gils<sup>\*</sup>,  
 R. Glasstetter<sup>\*\*</sup>, C. Grupen<sup>¶</sup>, D. Heck<sup>\*</sup>, J.R. Hörandel<sup>§</sup>,  
 K.-H. Kampert<sup>\*\*</sup>, H.O. Klages<sup>\*</sup>, Y. Kolotaev<sup>¶</sup>, G. Maier<sup>\*,2</sup>,  
 H.J. Mathes<sup>\*</sup>, H.J. Mayer<sup>\*</sup>, J. Milke<sup>\*</sup>, B. Mitrica<sup>†</sup>, C. Morello<sup>||</sup>,  
 M. Müller<sup>\*</sup>, G. Navarra<sup>‡</sup>, R. Obenland<sup>\*</sup>, J. Oehlschläger<sup>\*</sup>,  
 S. Ostapchenko<sup>\*,3</sup>, S. Over<sup>¶</sup>, M. Petcu<sup>†</sup>, T. Pierog<sup>\*</sup>, S. Plewnia<sup>\*</sup>,  
 H. Rebel<sup>\*</sup>, A. Risse<sup>††</sup>, M. Roth<sup>§</sup>, H. Schieler<sup>\*</sup>, O. Sima<sup>†</sup>,  
 M. Stümpert<sup>§</sup>, G. Toma<sup>†</sup>, G.C. Trincherio<sup>||</sup>, H. Ulrich<sup>\*</sup>,  
 S. Valchierotti<sup>‡</sup>, J. van Buren<sup>\*</sup>, W. Walkowiak<sup>¶</sup>, A. Weindl<sup>\*</sup>,  
 J. Wochele<sup>\*</sup>, J. Zabierowski<sup>††</sup>, S. Zagromski<sup>\*</sup>, and D. Zimmermann<sup>¶</sup>

<sup>\*</sup>Institut für Kernphysik, Forschungszentrum Karlsruhe, 76021 Karlsruhe, Germany

<sup>†</sup>National Institute of Physics and Nuclear Engineering, 7690 Bucharest, Romania

<sup>‡</sup>Dipartimento di Fisica Generale dell'Università, 10125 Torino, Italy

<sup>§</sup>Institut für Experimentelle Kernphysik, Universität Karlsruhe, 76021 Karlsruhe, Germany

<sup>¶</sup>Fachbereich Physik, Universität Siegen, 57068 Siegen, Germany

<sup>||</sup>Istituto di Fisica dello Spazio Interplanetario, CNR, 10133 Torino, Italy

<sup>\*\*</sup>Fachbereich Physik, Universität Wuppertal, 42097 Wuppertal, Germany

<sup>††</sup>Soltan Institute for Nuclear Studies, 90950 Lodz, Poland

E-mail: haungs@ik.fzk.de

**Abstract.** Recent results from the multi-detector set-up KASCADE on measurements of cosmic rays in the energy range of the so called "first" knee (at  $\approx 3$  PeV) indicate a distinct knee in the energy spectra of light primary cosmic rays and an increasing dominance of heavy ones towards higher energies. This leads to the expectation of knee-like features of the heavy primaries at around 100 PeV. To investigate this energy region KASCADE has recently been extended by a factor 10 in area to the new experiment KASCADE-Grande. Main results of KASCADE as well as set-up, capabilities, and status of KASCADE-Grande are presented.

## 1. Introduction

The all-particle energy spectrum of cosmic rays shows a distinctive discontinuity at few PeV, known as the knee, where the spectral index changes from  $-2.7$  to approximately  $-3.1$  (Fig. 1).

<sup>1</sup> on leave of absence from National Institute of Physics and Nuclear Engineering, 7690 Bucharest, Romania

<sup>2</sup> now at University Leeds, LS2 9JT Leeds, United Kingdom

<sup>3</sup> on leave of absence from Moscow State University, 119899 Moscow, Russia

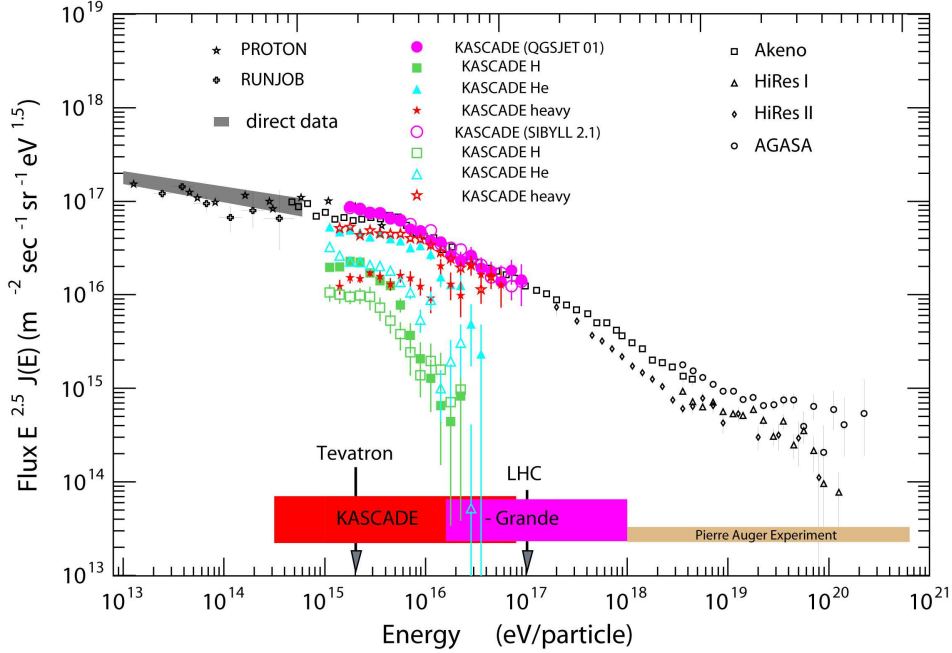


**Figure 1.** Primary cosmic ray flux and primary energy range covered by KASCADE-Grande. Results of the KASCADE data analyses are also shown (see text).

At that energy direct measurements are presently hardly possible due to the low flux, but indirect measurements observing extensive air showers (EAS) are performed. Astrophysical scenarios like the change of the acceleration mechanisms at the cosmic ray sources (supernova remnants, pulsars, etc.) or effects of the transport mechanisms inside the Galaxy (diffusion with escape probabilities) are conceivable for the origin of the knee as well as particle physics reasons like a new kind of hadronic interaction inside the atmosphere or during the transport through the interstellar medium. Two classes of theories (diffusion or acceleration based) predict knee positions occurring at constant rigidity of the particles. On the other hand, the hypothesis of new hadronic interaction mechanisms at the knee energy, as for example the production of heavy particles in  $pp$  collisions, implies an atomic mass dependence of the knee positions. It is obvious that only detailed measurements over the whole energy range of the knee from  $10^{14}$  eV to  $10^{18}$  eV and analyses of the primary energy spectra for the different incoming particle types can validate or disprove some of these models.

The highest cosmic energies above the so called ankle are believed to be of extragalactic origin. Thus, in the experimentally less explored region between the first ("proton") knee and the ankle there are two more peculiarities of the cosmic ray spectrum expected: (i) A knee of the heavy component which is expected (depending on the model) either at the position of the first knee times  $Z$  (the charge) or times  $A$  (the mass) of iron. (ii) A transition region from galactic to extragalactic origin of cosmic rays, where there is no theoretical reason for a smooth crossover in slope and flux.

Despite EAS measurements with many experimental setups in the last five decades the origin of the knee is still not clear, as the disentanglement of the threefold problem of estimate of energy and mass plus the understanding of the air-shower development in the Earth's atmosphere remains an experimental challenge. For a detailed discussion of the subject see the review in [1].

The multi-detector system KASCADE-Grande (KARlsruhe Shower Core and Array DETector

and Grande array) approaches this challenge by measuring as much as possible redundant information from each single air-shower event. The multi-detector arrangement allows to measure the total electron and muon numbers of the shower separately using an array of shielded and unshielded detectors. Additionally muon densities at further three muon energy thresholds and the hadronic core of the shower by an iron sampling calorimeter are measured. Recently, the original KASCADE experiment [2] was extended in area by a factor 10 to the new experiment KASCADE-Grande [3, 4, 5]. KASCADE-Grande allows now a full coverage of the energy range around the knee, including the possible second knee (see Fig. 1).

From KASCADE [2] measurements we do know that at a few times  $10^{15}$  eV the knee is due to light elements [6], that the knee positions depend on the kind of the incoming particle, and that cosmic rays around the knee arrive our Earth isotropically [7, 8]. KASCADE-Grande [3, 4], measuring higher energies, will prove, if existent, the knee corresponding to heavy elements. Additionally KASCADE could show that no current hadronic interaction model which are unavoidably needed for the interpretation of air shower data, describes very well cosmic ray measurements in the energy range of the knee and above [9, 10]. These model uncertainties are due to the lack of accelerator data at these energies and especially for the forward direction of collisions. Multi-detector systems like KASCADE and KASCADE-Grande offer the possibility of testing and tuning the different hadronic interaction models.

With its capabilities KASCADE-Grande is also the ideal testbed for the development and calibration of new air-shower detection techniques like the measurement of EAS radio emission [11].

The present contribution will summarize the main results of the KASCADE experiment and discuss the capabilities and status of KASCADE-Grande.

## 2. The KASCADE-Grande Experiment

The KASCADE-Grande experiment, located at the Forschungszentrum Karlsruhe, Germany, (49°n, 8°e, 110 m a.s.l.) measures showers in a primary energy range from 100 TeV to 1 EeV and provides multi-parameter measurements on a large number of observables concerning electrons, muons at 4 energy thresholds, and hadrons. The main detector components of KASCADE-Grande are the KASCADE Array, the Grande array, the Central Detector, and the Muon Tracking Detector (see Table 1).

The KASCADE Array measures the total electron and muon numbers ( $E_\mu > 230$  MeV) of the shower separately using an array of 252 detector stations containing shielded and unshielded detectors at the same place in a grid of  $200 \times 200$  m<sup>2</sup>. The excellent time resolution of these detectors allows also decent investigations of the arrival directions of the showers in searching large scale anisotropies and, if existent, cosmic ray point sources. The KASCADE array is optimized to measure EAS in the energy range of 100 TeV to 80 PeV.

The Muon Tracking Detector (128 m<sup>2</sup>) measures the incidence angles of muons ( $E_\mu > 800$  MeV) relative to the shower arrival direction. These measurements provide a sensitivity to the longitudinal development of the showers.

The hadronic core of the shower is measured by a 300 m<sup>2</sup> iron sampling calorimeter installed at the KASCADE Central Detector: Three other components - trigger plane (serves also as timing facility), multiwire proportional chambers (MWPC), and limited streamer tubes (LST) - offer additional valuable information on the penetrating muonic component at 490 MeV and 2.4 GeV energy thresholds, respectively.

The multi-detector concept of the KASCADE experiment (Fig. 2, which is operating since 1996 has been translated to higher primary energies through KASCADE-Grande [12].

The 37 stations of the Grande Array (Fig. 3) extend the cosmic ray measurements up to primary energies of 1 EeV. The Grande stations, 10 m<sup>2</sup> of plastic scintillator detectors each,

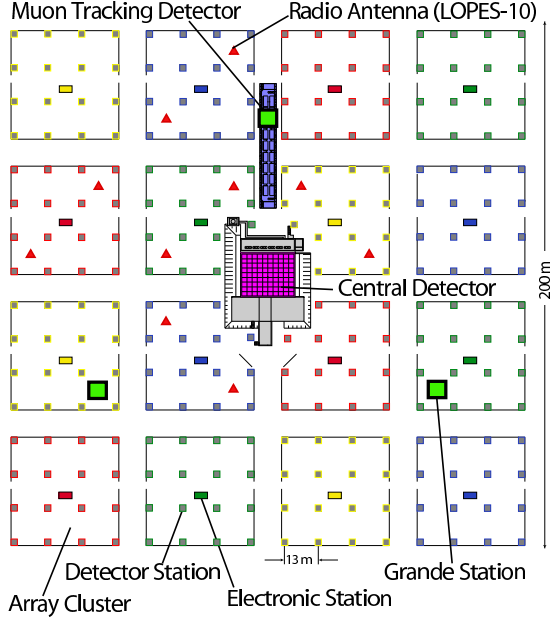


**Figure 2.** The main detector components of the KASCADE experiment: (the 16 clusters of) Field Array, Muon Tracking Detector and Central Detector. The location of 10 radio antennas is also displayed, as well as three stations of the Grande array.

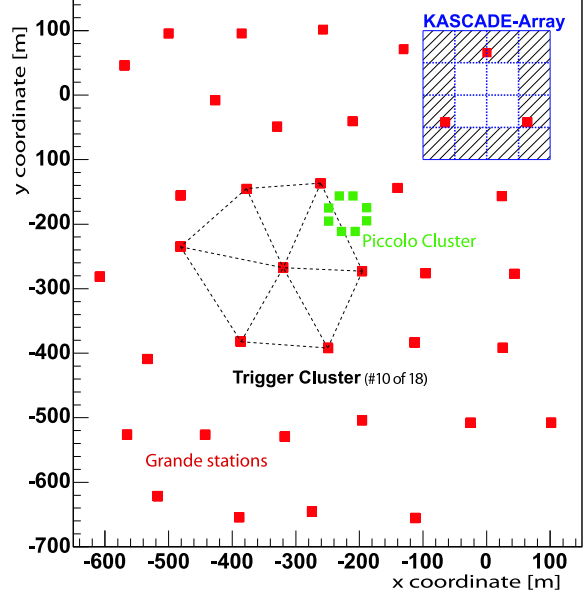


**Figure 3.** Layout of the KASCADE-Grande experiment with its 37 Grande and 8 Piccolo stations. One of the 18 Grande trigger hexagons is also shown.

**Table 1.** Compilation of the main KASCADE-Grande detector components. The threshold values are given for the particles kinetic energy.

Detector	Particles	sensitive area [m <sup>2</sup> ]
Grande	charged	370
Piccolo	charged	80
KASCADE array $e/\gamma$	electrons	490
KASCADE array $\mu$	muons ( $E_{\mu}^{\text{thresh}} = 230 \text{ MeV}$ )	622
MTD	muons ( $E_{\mu}^{\text{thresh}} = 800 \text{ MeV}$ )	$3 \times 128$
Trigger Plane	muons ( $E_{\mu}^{\text{thresh}} = 490 \text{ MeV}$ )	208
MWPCs/LSTs	muons ( $E_{\mu}^{\text{thresh}} = 2.4 \text{ GeV}$ )	$3 \times 129$
Calorimeter	hadrons ( $E_h^{\text{thresh}} = 10 - 20 \text{ GeV}$ )	$9 \times 304$
LOPES	radio wave (40 – 80 MHz)	30 dipole antennas

are spaced at approximative 130 m covering a total area of  $\sim 0.5 \text{ km}^2$ . There are 16 scintillator sheets in a station read out by 16 high gain photomultipliers; 4 of the scintillators are read out also by 4 low gain PMs. The covered dynamic range is up to 3000 mips/m<sup>2</sup>. A trigger signal is build when 7 stations in a hexagon (trigger cluster, see Fig. 3) are fired. Therefore, the Grande array consists of 18 hexagons with a total trigger rate of 0.5 Hz.

Additionally to the Grande Array a compact array, named Piccolo, has been build in order to provide a fast trigger to KASCADE ensuring joint measurements for showers with cores located far from the KASCADE array. The Piccolo array consists of 8 stations with 11 m<sup>2</sup> plastic

scintillator each, distributed over an area of  $360 \text{ m}^2$ . One station contains 12 plastic scintillators organized in 6 modules; 3 modules form a so-called electronic station providing ADC and TDC signals. A Piccolo trigger is built and sent to KASCADE and Grande when at least 7 out of the 48 modules of Piccolo are fired. Such a logical condition leads to a trigger rate of 0.3 Hz.

To improve further the data quality a self-triggering, dead-time free FADC-based DAQ system will be implemented in order to record the full time evolution of energy deposits in the Grande stations at an effective sampling rate of 250 MHz and high resolution of 12 bits in two gain ranges [13]. This will lead to an intrinsic electron-muon separation of the data signal at the Grande array.

The whole KASCADE-Grande setup is read out if a certain multiplicity of the KASCADE, Piccolo, or the Grande array detector stations or of the trigger plane is firing, leading to a total trigger rate of  $\approx 4.5 \text{ Hz}$ .

The redundant information of the showers measured by the Central Detector and the Muon Tracking Detector is predominantly being used for tests and improvements of the hadronic interaction models underlying the analyses [14].

For the calibration of the radio signal emitted by the air shower in the atmosphere an array of first 10 and meanwhile 30 dipole antennas (LOPES) is set up on the site of the KASCADE-Grande experiment [15].

### 3. KASCADE results

#### 3.1. Search for anisotropies and point sources

Investigations of anisotropies in the arrival directions of the cosmic rays give additional information on the cosmic ray origin and of their propagation. Depending on the model of the origin of the knee and on the assumed structure of the galactic magnetic field one expects large-scale anisotropies on a scale of  $10^{-4}$  to  $10^{-2}$  in the energy region of the knee. The limits of large-scale anisotropy analyzing the KASCADE data as shown in Fig. 4 are determined to be between  $10^{-3}$  at 0.7 PeV primary energy and  $10^{-2}$  at 6 PeV [7]. These limits were obtained by investigations of the Rayleigh amplitudes and phases of the first harmonics. Taking into account possible nearby sources of galactic cosmic rays like the Vela Supernova remnant [17] the limits of KASCADE already exclude particular model predictions.

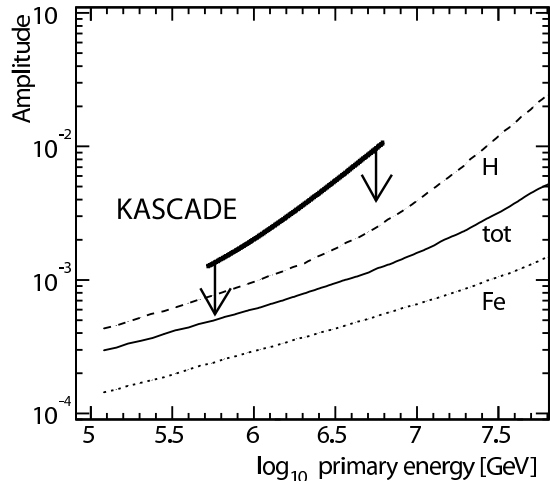


**Figure 4.** Rayleigh amplitude of the harmonic analyses of the KASCADE data [7] (limit on a 95% confidence level) compared to theory predictions [16].

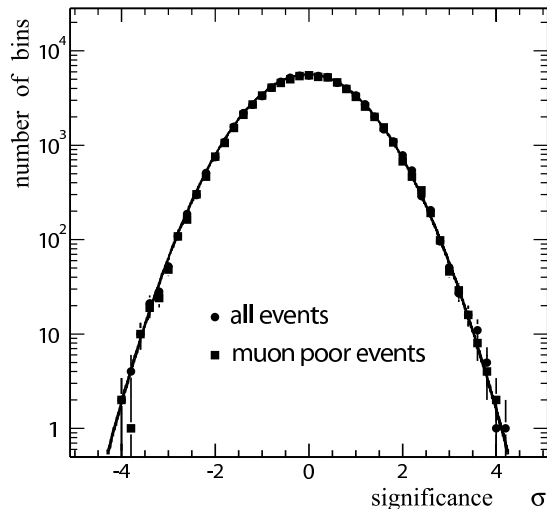


**Figure 5.** Significance distributions for searching point sources on the sky map seen by the KASCADE experiment [8].

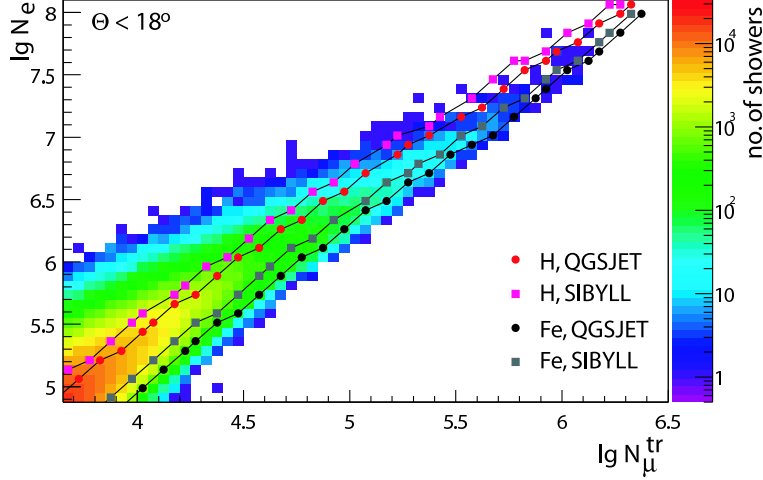


**Figure 6.** Two dimensional electron ( $N_e$ ) vs. muon ( $N_\mu^{\text{tr}}$  = number of muons in 40-200m core distance) number spectrum measured by the KASCADE array. The lines display the most probable values for proton and iron primaries obtained by CORSIKA simulations employing different hadronic interaction models.

The interest for looking to point sources in the KASCADE data sample arises from the possibility of unknown near-by sources, where the deflection of the charged cosmic rays would be small or by sources emitting neutral particles like high-energy gammas or neutrons. The scenario for neutrons is very interesting for KASCADE-Grande, since the neutron decay length at these energies is in the order of the distance to the Galactic center. In KASCADE case, the full sample of air showers were investigated as well as a sample of "muon-poor" showers which is a sample with an enhanced number of candidates of  $\gamma$ -ray induced events (Fig. 5). No significant excess was found in both samples [8].

### 3.2. Energy spectra of individual mass groups

The KASCADE data analyses aims to reconstruct the energy spectra of individual mass groups taking into account not only different shower observables, but also their correlation on an event-by-event basis. The content of each cell of the two-dimensional spectrum of reconstructed electron number vs. muon number (Fig. 6) is the sum of contributions from the individual primary elements. Hence the inverse problem  $g(y) = \int K(y, x)p(x)dx$  with  $y = (N_e, N_\mu^{\text{tr}})$  and  $x = (E, A)$  has to be solved. This problem results in a system of coupled Fredholm integral equations of the form

$$\frac{dJ}{d \lg N_e d \lg N_\mu^{\text{tr}}} = \sum_A \int_{-\infty}^{+\infty} \frac{dJ_A}{d \lg E} \cdot p_A(\lg N_e, \lg N_\mu^{\text{tr}} | \lg E) \cdot d \lg E$$

where the probability  $p_A$  is a further integral with the kernel function  $k_A = r_A \cdot \epsilon_A \cdot s_A$  factorized into three parts. The quantity  $r_A$  describes the shower fluctuations, i.e. the distribution of electron and muon number for given primary energy and mass. The quantity  $\epsilon_A$  describes the trigger efficiency of the experiment, and  $s_A$  describes the reconstruction probabilities, i.e. the distribution of reconstructed  $N_e$  and  $N_\mu^{\text{tr}}$  for given true numbers of electrons and muons. The probabilities  $p_A$  are obtained by Monte Carlo simulations on basis of two different hadronic interaction models (QGSJET 01 [18], SIBYLL 2.1 [19]) as options embedded in CORSIKA [20]. By applying the above described procedures (with the assumption of five primary mass groups, only) to the experimental data energy spectra are obtained as displayed in Figs. 7, 8 and in Fig. 1, where the resulting spectra for primary oxygen, silicon, and iron are summed up for a

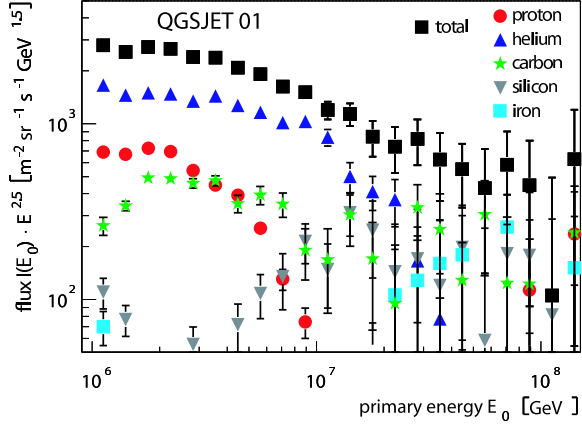


**Figure 7.** Result of the unfolding procedure based on QGSJET 01.

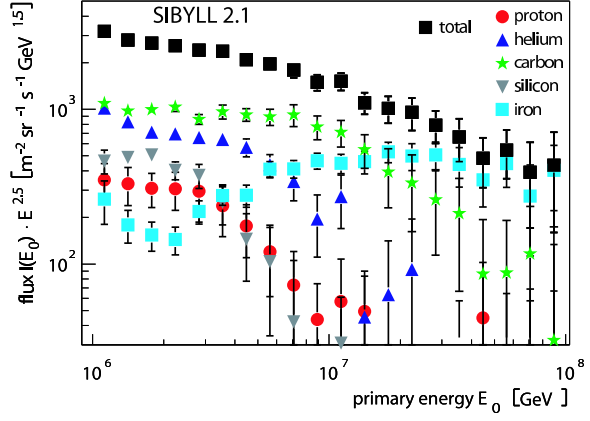


**Figure 8.** Result of the unfolding procedure based on SIBYLL 2.1.

better visibility.

A knee like feature is clearly visible in the all particle spectrum, which is the sum of the unfolded single mass group spectra, as well as in the spectra of primary proton and helium. This demonstrates that the elemental composition of cosmic rays is dominated by the light components below the knee and by a heavy component above the knee feature. Thus, the knee feature originates from a decreasing flux of the light primary particles [9, 10].

### 3.3. Inaccuracies of hadronic interaction models

Comparing the unfolding results based on the two different hadronic interaction models, the model dependence when interpreting the data is obvious. Modeling the hadronic interactions underlies assumptions from particle physics theory and extrapolations resulting in large uncertainties, which are reflected by the discrepancies of the results presented here. In Fig. 6 the predictions of the  $N_e$  and  $N_\mu^{tr}$  correlation for the two models are overlayed to the measured distribution in case of proton and iron primaries. It is remarkable that all four lines have a more or less parallel slope which is different from the data distribution. There, the knee is visible as kink to a flatter  $N_e$ - $N_\mu^{tr}$  dependence above  $\lg N_\mu^{tr} \approx 4.2$ . The heavier primary contribution on the results based on the SIBYLL model is due to predictions of a smaller ratio of muon to electron number for all primaries. Comparing the residuals of the unfolded two dimensional distributions for the different models with the initial data set we conclude [10] that at lower energies the SIBYLL model and at higher energies the QGSJET model are able to describe the correlation consistently, but none of the present models gives a contenting description of the whole data set. These findings are confirmed by detailed investigations of further shower observables measured by KASCADE [14].

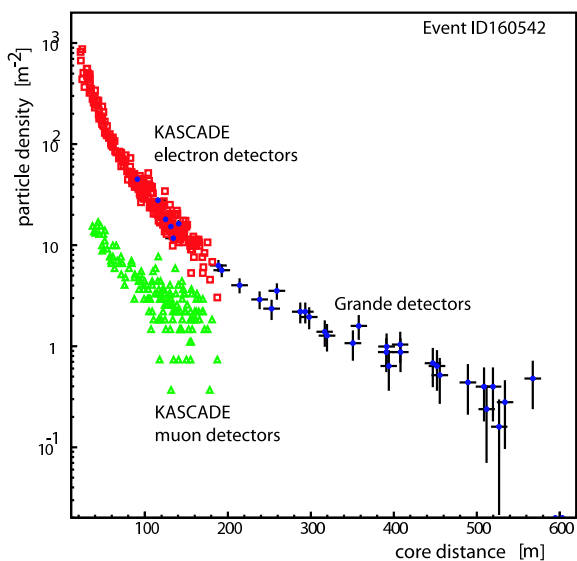
Crucial parameters in the modeling of hadronic interaction models which can be responsible for these inconsistencies are the total nucleus-air cross-section and the parts of the inelastic and diffractive cross sections leading to shifts of the position of the shower maximum in the atmosphere and, therefore, to a change of the muon and electron numbers as well as to their correlation on single air shower basis. The multiplicity of the pion generation at all energies at the hadronic interactions during the air shower development is also a 'semi-free' parameter in the air-shower modeling as accelerator data have still large uncertainties, in particular for the forward direction [21].



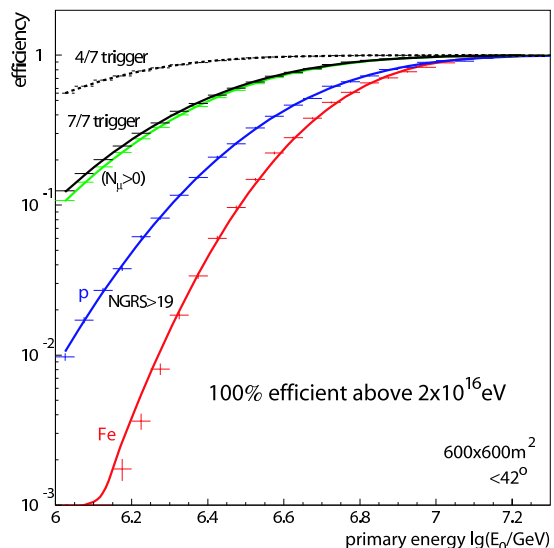
#### 4. Status, capabilities and perspectives of KASCADE-Grande

Fig. 9 shows, for a single event, the lateral distribution of electrons and muons reconstructed with KASCADE and the charge particle densities measured by the Grande stations. This example illustrates the capabilities of KASCADE-Grande and the high quality of the data. The KASCADE-Grande reconstruction procedure follows iterative steps: shower core position, angle-of-incidence, and total number of charged particles are estimated from Grande Array data; the muon densities and with that the reconstruction of the total muon number is provided by the KASCADE muon detectors. The reconstruction accuracy (Fig. 11) of the shower core position and direction is in the order of 4 m (13 m) and  $0.18^\circ$  ( $0.32^\circ$ ) with 68% (95%) confidence level for proton and iron showers at 100 PeV primary energy and  $22^\circ$  zenith angle [22]. The statistical uncertainty of the shower sizes are around 10 – 15% and 20 – 25% for the total numbers of electrons and muons, respectively. The critical point of the KASCADE-Grande reconstruction is the estimation of the muon number due to the limited sampling of the muon lateral distribution by the KASCADE muon detectors. The systematic uncertainty for the muon number depends on the radial range of the data measured by the KASCADE array and the chosen lateral distribution function.

At the KASCADE experiment, the two-dimensional distribution shower size - truncated number of muons played the fundamental role in reconstruction of energy spectra of single mass groups. In Figure 12 the correlation of these two shower sizes for both cases KASCADE and



**Figure 9.** Particle densities in the different detector types of KASCADE-Grande measured for a single event.



**Figure 10.** Efficiency of the Grande array (details see text). CORSIKA simulations including detailed simulation of the detector response.

KASCADE-Grande measurements are compared for a 1-day test-run. For the same run time, due to its 10 times larger area compared with KASCADE, the Grande Array sees a significant number of showers at primary energies  $\sim 10$  times higher. Hence, Figure 12 illustrates the capability of KASCADE-Grande to perform an unfolding procedure like in KASCADE.

Figure 10 shows the efficiency characteristics of the KASCADE-Grande array. For internal tests of the detector stations a 4/7 trigger is performed at the hexagons. The efficiency of the 7/7 trigger is also shown which is only marginal smaller if the additional requirement is imposed

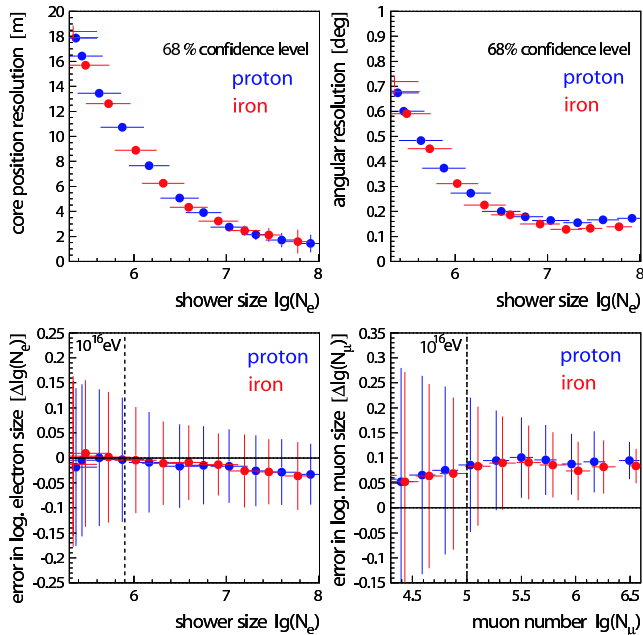


**Figure 11.** Core, angular, and shower size reconstruction resolution of the KASCADE-Grande experiment. CORSIKA simulations including detailed simulation of the detector response.

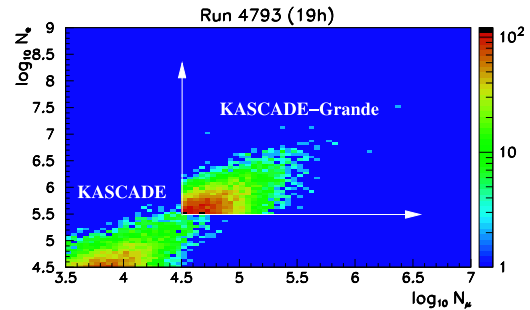


**Figure 12.** Comparison between KASCADE and KASCADE-Grande data for a combined test-run.

that the muon number has to be reconstructed with the information of the muon detectors of the original KASCADE array. To reduce efficiently the amount of data a software cut will be applied with the requirement of at least 20 Grande stations ( $NGRS > 19$ ) have to be fired. A hundred percent efficiency is then reached for all primary particle types for energies above  $2 \cdot 10^{16}$  eV, providing still a large overlap with the KASCADE energy range. The limit at high energies for Grande is due to the limitation in area and not saturation of the detectors, as even at primary energy of  $10^{18}$  eV only one station in average is saturated.

KASCADE-Grande started end of 2003 with combined measurements of all detector components. Currently (spring 2005) a FADC system is installed at the Grande stations which will run in parallel to the present data acquisition. Besides the physics gain with the possible intrinsic separation of electrons and muons by having the full shower time history, this additional information will be used for cross-checking the calibration procedures of KASCADE-Grande.

## 5. Conclusions

The extension of KASCADE to the KASCADE-Grande experiment, accessing higher primary energies, is expected to solve the question of the existence of a knee-like structure corresponding to heavy elements. KASCADE-Grande keeps the multi-detector concept for tuning different interaction models at primary energies up to  $10^{18}$  eV. KASCADE-Grande also provides the perfect environment detecting radio emission in extensive air showers, which is the aim of the LOPES project [23].

## Acknowledgments

KASCADE-Grande is supported by the Ministry for Research and Education of Germany, the INFN of Italy, the Polish State Committee for Scientific Research (KBN grant for 2004-06) and the Romanian National Academy for Science, Research and Technology.

- [1] Haungs A, Rebel H, and Roth M 2003 *Rep. Prog. Phys.* **66** 1145
- [2] Antoni T et al. - KASCADE collaboration 2003 *Nucl. Instr. Meth. A* **513** 429
- [3] Navarra G et al. - KASCADE-Grande collaboration 2004 *Nucl. Instr. Meth. A* **518** 207
- [4] Haungs A et al. - KASCADE-Grande collaboration 2003 *Proc. of 28<sup>th</sup> ICRC, Tsukuba, Japan* p.985.
- [5] Haungs A et al. - KASCADE-Grande collaboration 2004 *Proc. 22<sup>nd</sup> Texas Symposium, Stanford, CA, Dec. 2004* eConf **C041213** 2414
- [6] Antoni T et al. - KASCADE collaboration 2002 *Astrop. Phys.* **16** 373
- [7] Antoni T et al. - KASCADE collaboration 2004 *Astrophys. J.* **604** 687
- [8] Antoni T et al. - KASCADE collaboration 2004 *Astrophys. J.* **608** 865
- [9] Antoni T et al. - KASCADE collaboration 2005 *Astrop. Phys.* in press, astro-ph/0505413
- [10] Ulrich H et al. - KASCADE collaboration 2004 *Europ. J. C* DOI 10.1140/epjcd/s2004-03-1632-2
- [11] Horneffer A et al. - LOPES collaboration 2004 *Proc. SPIE* **5500** 129
- [12] Badea A F et al. - KASCADE-Grande collaboration 2004 *Nucl. Phys. B (Proc. Suppl.)* **136** 384
- [13] Walkowiak W et al. - KASCADE-Grande collaboration 2004 "A FADC-based Data Acquisition System for the KASCADE-Grande Experiment", *Proc. of IEEE Nuclear Science Symposium, Rome*
- [14] Haungs A et al. - KASCADE collaboration 2005 *Proc. XIII ISVHECRI 2004, Pylos, Nucl. Phys. B (Proc. Suppl.)* in press, astro-ph/0412610
- [15] Haungs A et al. - LOPES collaboration 2004 *Proc. 22<sup>nd</sup> Texas Symposium, Stanford, CA, Dec. 2004* eConf **C041213** 2413
- [16] Candia J et al. 2003 *Astrop. Phys.* **5** 3
- [17] Ptuskin V 1996 *Adv. in Space Res.* **19** 697
- [18] Kalmykov N N, Ostapchenko S S 1993 *Phys. Atom. Nucl.* **56** 346
- [19] Engel R et al. 1999 *26<sup>th</sup> ICRC, Salt Lake City, Utah* p.415
- [20] Heck D et al. 1998 *Report FZKA 6019, Forschungszentrum Karlsruhe*
- [21] Engel R 2003 *Nucl. Phys. B (Proc. Suppl.)* **122** 437
- [22] Glasstetter R et al. - KASCADE-Grande collaboration 2003 *Proc. of 28<sup>th</sup> ICRC, Tsukuba, Japan* p.781
- [23] Falcke H et al. - LOPES collaboration 2005 *Nature* **435** 313